

## DYNAMICS AND STRUCTURE OF FLUID FLOWS: OBSERVATIONS AND CALCULATIONS

Yuli D. Chashechkin<sup>1</sup>,

<sup>1</sup> Laboratory of Fluid Mechanics, A.Yu.Ishlinskiy Institute for Problems in Mechanics of the RAS, 101/1 prospect Vernadskogo, Moscow 119526, Russia

### Abstract

Fine structure of stratified flows observed in laboratory with schlieren instruments is calculated using supercomputers on basis of the fundamental equations set. Two kind of stratified flows are analysed: diffusion induced flows on motionless strip and flow around uniformly moving strip. Data of calculations and laboratory experiments are well compatible.

**Keywords:** stratified flows, calculation, observation

### 1 Introduction

Modern optical instruments revealed spatially ordered structures of different scales from light-years length in the interstellar medium to microns in the laboratory. Regular radial structures were observed in the images of the Red giant in the constellation Camelopardalis and in drying drops of diluted suspension of quartz nanoparticles in alcohol with thickness of fifty microns [1]. Thin streaky structures are formed in the tank filled with a dilute suspension of aluminium powder during parametric excitation of standing waves [2]. Compact spot of a solvable dye on the surface of the compound vortex expands into spiral arms that gradually disintegrate into individual filaments [3]. Unlike liquid, solid markers are not only transported by a vortex flow, but also are swirling around their own centres [4]. Wide range of scales of streaky structures indicates universal nature of their formation and the need to develop a general mathematical model of the process.

Modern theories are constructed for describing both dynamics and the fine structure of environmental and industrial flows and pointing indicating directions for development of the perspective experimental technique and data processing. Conventional basis for universal theory is complete set of balance equations representing fundamental laws of conservation for dissipative fluids. All basic equations including continuity, momentum, complete energy and constituents of the fluid components balance equations were postulated in XIX century. They were collected together and presented in the main textbooks, starting from volume 3 of Landau's and Lifshitz's seminal course [5].

### 2. Fundamental equations set.

Collected together and supplemented by the state equation basic differential equations form the fundamental set, defining the “fluid flow” as a transport of momentum accompanied by self-consistent variations of density, energy (temperature) and concentrations of dissolved matter. The set contains only observable physical quantities such as momentum  $\mathbf{p}$  and basic thermodynamic parameters that are density  $\rho$ , pressure  $P$ , entropy (internal energy or temperature  $T$ ), concentration (salinity  $S$ ), which can be measured by different independent methods. For example momentum  $\mathbf{p}$  can be defined from independent measurements of the flow rate and forcing action of the flow on a small obstacle.

The fundamental equation set describing flows of a compressible stratified and generally rotating fluid in the Euclidean coordinate frame includes empiric equations of state, differential equations of continuity, balance of momentum, temperature, salinity and has the form

$$\rho = \rho(P, S, T), \quad (1)$$

$$\frac{\partial \rho}{\partial t} + \nabla_j (p_j) = 0 \quad (2)$$

$$\frac{\partial (p_j)}{\partial t} + \left( \nabla_j \frac{p_j}{\rho} \right) p_i = -\nabla_i P + \rho g_i + \nu \Delta \left( \frac{p_j}{\rho} \right) + 2\varepsilon_{ijk} p_j \Omega_k + f_i \quad (3)$$

$$\frac{\partial \rho T}{\partial t} + \nabla_j \cdot (p_j T) = \Delta (\kappa_T \rho T), \quad (4)$$

$$\frac{\partial \rho S}{\partial t} + \nabla_j \cdot (p_j S) = \Delta (\kappa_S \rho S) \quad (5)$$

Here  $\rho$  is density,  $p_i$  are components of momentum vector,  $v_j = p_j / \rho$  is a flow velocity,  $\Omega_k$  is angular velocity,  $g_i$  is gravity acceleration,  $f_i$  is external force,  $\nu$ ,  $\kappa_T$ ,  $\kappa_S$  are dissipative coefficients of kinematic viscosity, temperature conductivity and diffusivity. Direct calculations have shown that the set (1) is characterized by continuous ten-parametric Galilean groups [6]. Velocity of fluids is non-conservative derivative parameter and can be calculated in a given point of the flow as ratio of momentum to density of the fluid  $\mathbf{v} = \mathbf{p} / \rho$ . Due to independence of basic physical quantities like momentum and density in fluid flows geometry of momentum and velocity fields are not identical. So the *flow* cannot be defined as *motion* that is as transformation of the 3D Euclidean space into itself saving distances between objects.

For applied purposes besides the fundamental equations set innumerous number of reduced and constitutive equations were proposed during last century. The row of models includes different versions of turbulence and boundary layer theories, gas dynamics equations, linear and different non-linear equations and sets [5]. ~~The~~ every system is characterized by its own set of symmetries illustrating specific laws of conservation. Constitutive and reduced models are characterized by expanded or reduced groups of symmetries [6]. Change in symmetries indicates essential difference in properties of models and their solutions. Difference of symmetries also means that compared sets are not reducible and cannot be identically transformed into each other and the same symbols in different systems have different meaning.

### 3. Basic length scales of the set.

The rank of the non-linear set (1–5), order of its linear version and degree of algebraic characteristic equations (or dispersion relation for wave processes) is defined by the condition of compatibility. The system (1) supplemented by appropriate initial and boundary conditions is characterized by a number of distinguished length scales of two types. Large scales characterize initial or boundary conditions and includes geometrical length of the problem  $L$ , scale of stratification  $\Lambda_p = |d \ln \rho / dz|^{-1}$  and so on. Natural scale of time is buoyancy  $T_b = 2\pi / N$  or rotation  $T_r = 2\pi / \Omega_r$  period ( $N$ ,  $\Omega_r$  are appropriate frequencies).

Derivative scales are produced from the set of physical parameters of the problem like gravity wave length for attached surface  $\lambda_g = U^2 / g$  and  $\lambda_i = 2\pi U \sqrt{\Lambda / g}$  for internal gravity waves ( $U$  is typical velocity). A set of small scales is defined by dissipative coefficients and typical frequencies (buoyancy  $N$  or global rotation  $\Omega$ )  $\delta_N^v = \sqrt{v/N}$ ,  $\delta_N^{\kappa_T} = \sqrt{\kappa_T/N}$ ,  $\delta_N^{\kappa_s} = \sqrt{\kappa_s/N}$  or  $\delta_\Omega^v = \sqrt{v/\Omega}$ ,  $\delta_\Omega^{\kappa_T} = \sqrt{\kappa_T/\Omega}$ ,  $\delta_\Omega^{\kappa_s} = \sqrt{\kappa_s/\Omega}$  or the problem velocity  $\delta_U^v = v/U$  and  $\delta_U^{\kappa_s} = \kappa_s/U$ . The first scales are similar the Stokes length scale  $\delta_\omega^v = \sqrt{v/\omega}$  on an oscillating plane [1]. The second type scales that are Prandtl's and Peclet's type  $\delta_U^v = v/U$ ,  $\delta_U^{\kappa_T} = \kappa_T/U$ ,  $\delta_U^{\kappa_s} = \kappa_s/U$  characterize a fine structure in jets and wakes. Usually values of large and small scales are distinguished on several orders of magnitude.

There are also combined scales like dissipative gravity scale  $L_v = \sqrt[3]{g v / N}$  characterizing critical conditions for the problem geometry change. Multiplicity of intrinsic scales reflects complex nature of the fluid flows. Large number of intrinsic scales is related with the high dimension of the problem in the extended space. In experiments macroscales determine the size of the visualizing view field, which should contain all the components of flows and micro – scales define temporal and spatial resolution of the measuring and recording instruments.

Macro- and micro-scale relationships that define traditional dimensionless complexes that are Reynolds  $Re = UL/v = L/\delta_U^v \gg 1$  and Peclet numbers on temperature and salinity  $Pe_T = UL/\kappa_T = L/\delta_U^{\kappa_T} \gg 1$ ,  $Pe_s = UL/\kappa_s = L/\delta_U^{\kappa_s} \gg 1$ . These ratios are large in the environment and laboratory experiments. In most cases, the change in density of the flow scale is small and values of length scale  $C = \Lambda/L = \rho_0/\delta\rho \gg 1$  as dissipative relations  $C_N^v = L/\delta_N^v = \sqrt{L^2 N/v} \gg 1$  with the kinematic viscosity, thermal diffusivity  $C_N^{\kappa_T}$ , or substance diffusion  $C_N^{\kappa_s}$  are large. The presence of large relationships in the system with small coefficients in the terms with the highest derivatives justifies the possibility of singular perturbation theory to calculate a wide range of processes, primarily slow flows such as diffusion induced by topography or internal waves.

The compatibility condition defines the **rank** of non-linear set, the **order** of its linearized version and **degree** of algebraic characteristic (dispersion) equations that is a total or minimal (for non-linear set) number of independent functions constituting complete solution. In fluids with small dissipative coefficients complete classifications of infinitesimal periodic flows components describing besides the waves a fine flow structure were given [7]. It is shown that the number of regularly perturbed solutions of basic governing equations systems and its reduced versions when effect of one or more dissipative factor are ignored up to the approximation of ideal fluid remains constant and equal two [9].

The number of fine flow components described by singular perturbed solutions decreases from eight in the complete model to two when only viscosity effects are saved as well as density stratification. Two different fine flow components in viscous homogeneous fluid became identical. Merging of these initially different components means the degeneration of the given set and insolubility of the problem of calculating the three-dimensional flows of a homogeneous fluid. Using different kinds of fluids that are stratified with evident buoyancy effects ( $N \sim O(1) s^{-1}$ ), weakly stratified (potentially

homogeneous  $N \sim o(10^{-5}) \text{ s}^{-1}$ ) and actually homogeneous fluid of constant density ( $N \equiv 0$ ) gives a room for objective control of accuracy of numerical codes.

In flows a mechanical energy is transported by large-scale components. Energy dissipation and vorticity are associated with the fine-structure components. Contrast of the flow pattern is underlined by contaminants which are accumulated on interfaces. Condition of all component of different scales registration imposes additional requirements on experimental techniques concerning temporal and spatial resolution.

Loci of fine flow components depend on geometry and energy of the processes. They exist in all flows as slow like waves or diffusion induced flows on obstacles and in a fast jets and wakes. To calculate their properties the complete solutions of equation (1) set must be constructed. There are no universal methods for solutions the complex non-linear set (1) is treated numerically or reducing solvable form. In case of very low velocities and weak dissipative factors the set (1) is investigated by mixed analytical and numerical methods. As impressive example of a slow flow structure the diffusion induced flows on a finite size obstacle are selected. They are formed by buoyancy forces created by irregularities of stratification caused by the interruption of the diffusion flux in the environment on an impermeable obstacle.

#### 4. Diffusion induced flows on obstacles.

Diffusion-induced flows play a key role in the processes of mixing and passive substance transport and also in the formation of stratified medium fine structures. Such flows may lead to the formation of intensive valley and mountain winds in a stably stratified atmosphere and density flows in oceans. A number of physical processes are essentially influenced by diffusion-induced flows, including processes such as the melting of icebergs, the migration of tectonic plates and the transport of minerals and plankton. It may also trigger a propulsion mechanism, which leads to the self-movement of neutral buoyancy solids with special shapes inside a stably stratified ocean.

Numerical solution of set (1) where temperature effects were neglected was constructed using the open software package OpenFOAM. The developed algorithm works in all ranges of problem parameters corresponding to laboratory, atmosphere and hydrosphere conditions, including zero angles of inclination of the impermeable surface to horizon when conditions of existence of stationary asymptotic stationary solutions are violated.

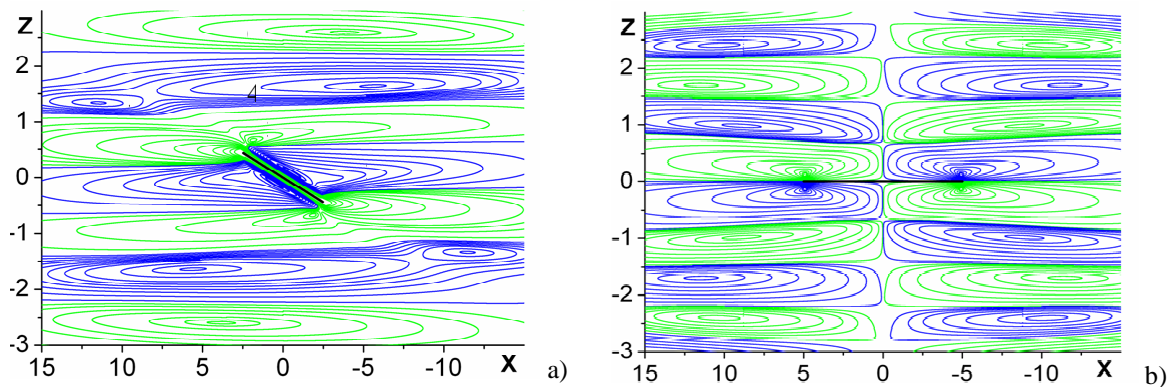


Figure 1: Pattern of streamlines of diffusion induced flows on the plate ( $L = 5 \text{ cm}$  ;  $N = 1.26 \text{ s}^{-1}$ ):

a) – sloping at  $\varphi = 10^\circ$  ; b) – horizontal  $\varphi = 0^\circ$  .

Calculations showed individual patterns of various physical parameters of the problem, part of which is represented in Figure 1. In the flow patterns of streamlines thin interfaces separate a number of regular cells (1 - 6 in Figure 1, *a*, positive direction by rotating marked green). Above the horizontal plate cells of different signs are located oppositely relative to the principal planes (Figure 1, *b*).

Even more clearly the fine structure of the flow is expressed in fields of the pressure perturbations (Figure 2, *a*). Along the plate surface a thin layer of the pressure deficit of non-uniform thickness is located. The most pronounced pressure perturbations are presented on the upper side near lower end of the plate and on the lower side near upper end. Mutual actions of the pressure deficit create the angular moment turning free plate of neutral buoyancy to horizontal position when diffusion induced flows have maximum value for given geometry of the obstacle.

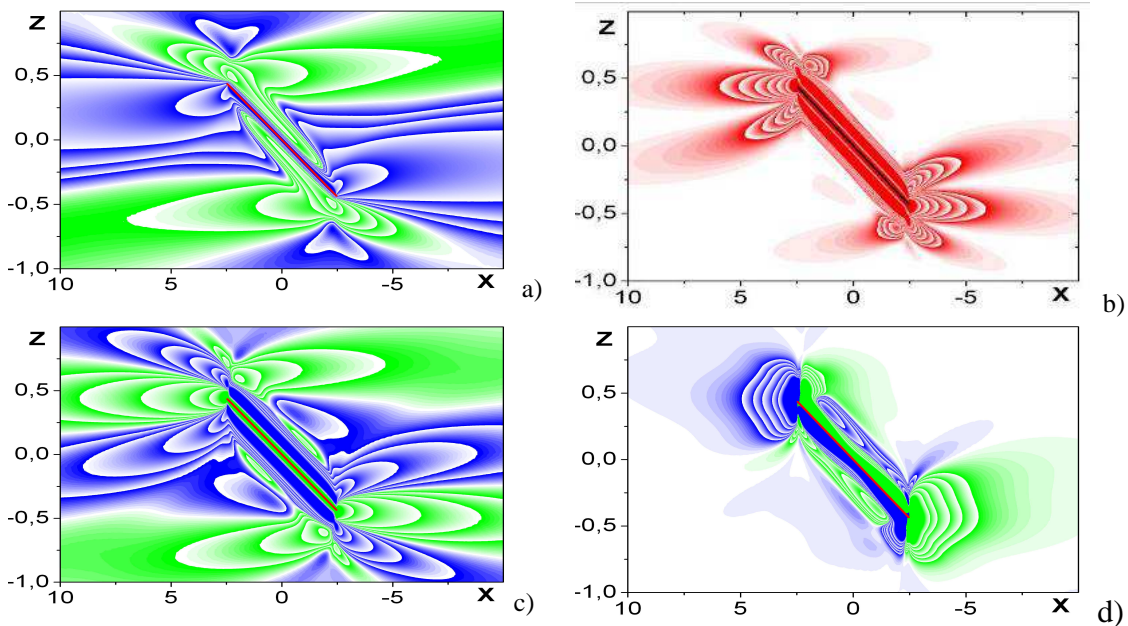


Figure 2: Fields of disturbances around the plate with length  $L = 5$  cm inclined under angle  $\varphi = 10^\circ$  to horizon: *a*) – pressure; *b*) – the rate of energy dissipation  $\epsilon$ ; *c*) – dynamic vorticity  $\Omega$ ; *d*) – tempo of baroclinic generation of vorticity  $\dot{\Omega}$  ( $N = 1.26 \text{ s}^{-1}$ ,  $\tau = t/T_b = 120$ , different scales on the axes).

Complex pattern of the rate of dissipation of mechanical energy (Figure 2, *b*) differs significantly from the smooth field of streamlines and the pressure field. Spatial structure of the mechanical energy dissipation rate  $\epsilon$  has specific "rosettes" shape at the ends of the plate which is typical for pattern of dissipative gravity waves or "zero frequency" waves. In pattern of the dynamical vorticity field  $\Omega = \text{rot } \mathbf{v} = \{0, \Omega, 0\}$  thin layer of the counter clockwise circulation adjusted to the plate surface is bounded by more thicker layer of clockwise circulation created in complex flow domain near the plate tips (Figure 2, *c*). Due to crossing of isopycnals and isobars additional vorticity is generated and in the close vicinity and at some distance from the obstacle with tempo  $\dot{\Omega} = \nabla P \times \nabla \rho^{-1}$  (Figure 2, *d*). The formation of new fine components in the vicinity of the edges of the plate is caused by the combined action of buoyancy, limiting the lifting height of separating jets streams, viscosity and diffusivity effects.

The calculated field of the density gradient perturbation for the diffusion induced flow on a horizontal or inclined plate, which manifest and large-scale components, the size of which is defined by the size of obstacle, and thin interfaces with scales  $\delta_N^v = \sqrt{v/N}$  or  $\delta_N^{\kappa_s} = \sqrt{\kappa_s/N}$ , at long times consistent with the schlieren image (“natural rainbow method” with a horizontal slit and regular grating) of the refractive index gradient near the plate in a laboratory tank (Figure 3, *a, b*).

In the images in Figure 3 stand out extensive streaky structures which are directly adjacent to the extreme points of the obstacles. The length of the interfaces increases with the sensitivity of the method of registration. Flow indicated by diffusion, lead to self-induced motion of free neutral buoyancy obstacles in a stratified medium with arbitrary geometry constraints and its orientation in space. Self-motion of obstacles is absent in a homogeneous fluid. Calculated velocities of fluid, the forces and angular moments acting on the wedge, consistent with the data of direct measurements of the velocity of self-motion of free neutral buoyancy wedge in a laboratory tank.

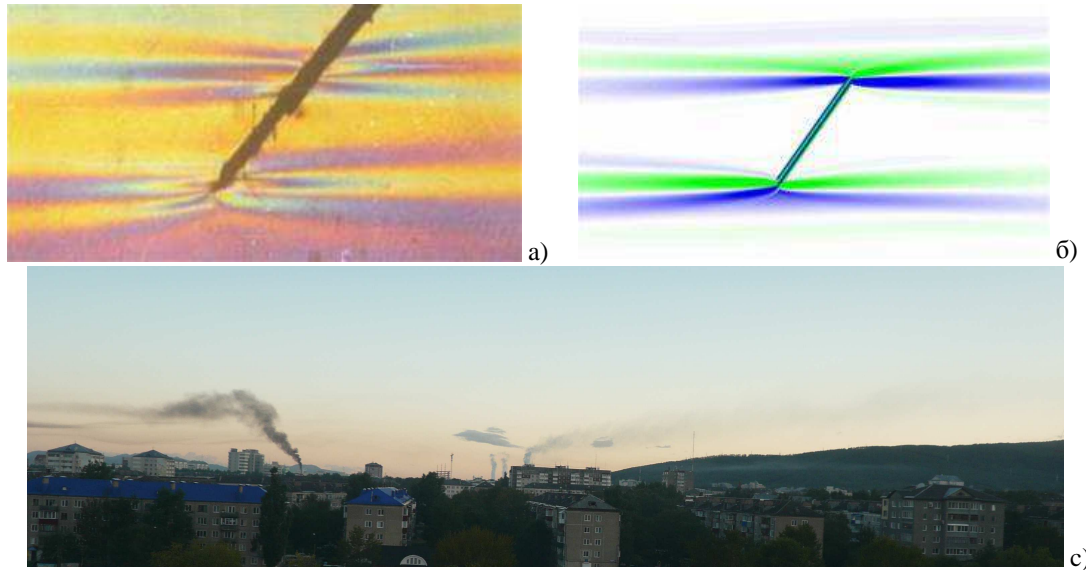


Figure 3: Images of diffusion induced flows: *a, b*) – schlieren and numeric visualization for laboratory condition of density gradient perturbations in the diffusion induced flow on sloping motionless strip ( $L = 5 \text{ cm}$ ,  $N = 0.84 \text{ s}^{-1}$ ,  $T_b = 7.5 \text{ s}$ ,  $\varphi = 40^\circ$ ); *c*) – smokes in Yuzhno-Sakhalinsk valley.

The overall pattern of the flow in the cavity (double vortex and sinking jet over the center and radiating stripe flows along the valley slopes) is preserved in the case of real atmospheric processes. As an example of the diffusion induced flow pattern in the atmosphere in Figure 3, *c* photograph at first glance paradoxical picture of industrial smokes in Yuzhno-Sakhalinsk is given.

## 5. 2D mathematical model of flow past a horizontal plate for $\text{Re} < 10^5$ .

With beginning of the plate motion the flow pattern around a plate changes radically. Internal waves and vortices are formed together with thin density wake. The set (1) were used for flow around the plate calculations together with the conventional boundary conditions that are no-slip for velocity components and no-flux for substance on the obstacle surface and attenuation of all perturbations at infinity [7]

$$v_x|_{\Sigma} = 0, \quad v_z|_{\Sigma} = 0, \quad \left[ \frac{\partial s}{\partial n} \right]_{\Sigma} = \frac{1}{\Lambda} \frac{\partial z}{\partial n}, \quad v_x|_{x, z \rightarrow \infty} = U_0, \quad v_z|_{x, z \rightarrow \infty} = 0.$$

The problem was analysed numerically using the finite volume method realized in original solvers of own development of the free distributed OpenFOAM package. The computations were run in parallel regime based on domain decomposition method using the facilities of the Joint Supercomputer Centre of the Russian Academy of Sciences and the Supercomputing Centre of Lomonosov Moscow State University.

When describing features of flow structure and dynamics around a horizontal plate several basic flow regimes should be distinguished. They include motionless state of the obstacle ( $Re = 0$ ), small ( $Re < 10^3$ ), moderate ( $10^3 < Re < 2 \cdot 10^4$ ) and relatively high ( $2 \cdot 10^4 < Re < 10^5$ ) speeds of plate motion, each of which is characterized by its own set of flow structural elements. To estimate quality of codes separate calculations for strongly stratified and weakly stratified fluids, potentially and actually homogeneous fluids have been performed with the same initial and boundary conditions.

Fields of diffusion induced flows on a motionless obstacle are used for construction of initial conditions in problems of real stratified flows dynamics and technological applications.

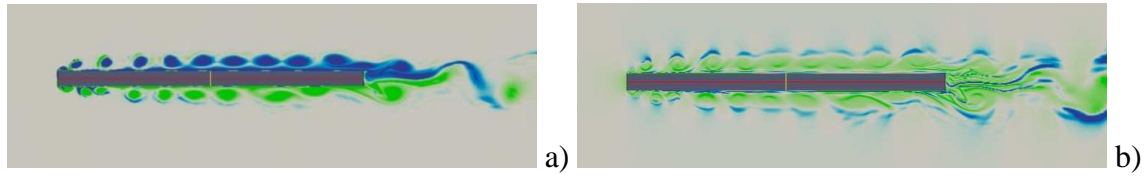


Figure 4: Patterns of vorticity and vertical component of density gradient fields of stratified flow around a horizontal plate:  $L = 10$  cm,  $h = 0.5$  cm,  $N = 1.2 \text{ s}^{-1}$ ,  $Re = 8 \cdot 10^4$

With start of plate movement initially symmetric structure of diffusion induced flow on a horizontal plate is changed and internal attached waves, upstream perturbations and vortex rolls being formed. Sources of internal waves are edges of the plate which generate intensive vertical displacement of fluid from initial positions of neutral buoyancy that results in formation of periodic fluid oscillations with decaying amplitudes.

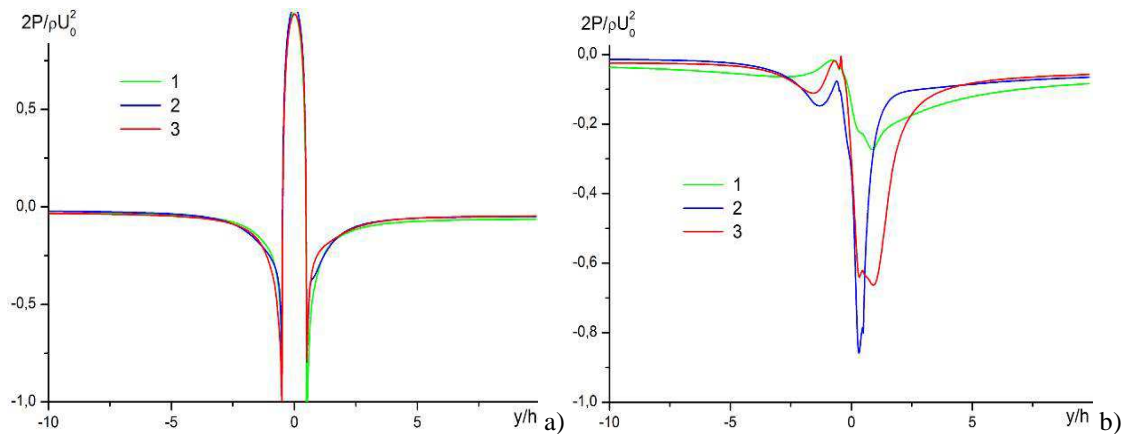


Figure 5: Normalized pressure profiles at the leading (a) and trailing (b) edges of the plate for different types of fluids: curves 1 – 3):  $N = 1.2; 10^{-5}; 0 \text{ s}^{-1}$ .

More details on stratified flow structure and dynamics around a horizontal plate at small and moderate Reynolds numbers can be found in [9]. In the case of relatively high Reynolds numbers the most manifested flow components in a stratified medium are both vortex structures generated by the sharp front edge of the plate and a vortex wake past the obstacle (Figure 4). Stratified flow structure evolves over time with downstream speed of vortical structures along the plate surface of about  $0.4U_0$ .

Instantaneous normalized pressure distributions across the stream at the front and trailing edges of the plate are shown in Figure 5 for strongly and weakly stratified, potentially and actually homogeneous fluids. The greatest differences of the profiles for different types of fluids are observed near the trailing edge of the plate where the vortex dynamics is the most intensive. Stratification effects like vortex shedding are determined by vertical dimension of an obstacle, which sets pressure, density and velocity gradients. So, in the considered case of a rather thick plate the stratified flow turns to be more sensitive to either direct or indirect effects of buoyancy forces.

General questions of fluid flows theory, conditions of resolvability and classification of flow components following from analysis of the fundamental governing equations sets are discussed in [10].

**Acknowledgements.** The work was partly supported by the Russian Academy of Sciences (Program 15OE-12 DEMBMCP RAS) and the RFBR (grant 15-01-09235).

## References

- [1] Chashechkin, Yu. D. & Bardakov, R. N.: Formation of texture in residue of a drying drop of a multicomponent fluid. *Doklady Physics*, Vol. 55, No. 2. (2010) pp. 68–72.
- [2] Chashechkin, Yu. D. & Kalinichenko, V.A.: Topographic patterns in the suspension structure in standing waves. *Doklady Physics*, Vol. 57, No 9. (2012) pp. 363–366.
- [3] Stepanova, E. V. & Chashechkin, Yu. D.: Marker transport in a composite vortex. *Fluid Dynamics*, Vol. 45, No. 6. (2010) pp. 843–858.
- [4] Budnikov, A. A., Zharkov, P. V. & Chashechkin, Yu. D. Experimental modeling of the shifting of floating objects in “garbage islands” *Moscow University Physical Bulletin*, Vol. 67, No. 4. (2012) pp. 403–408.
- [5] Landau, L.D. & Lifshitz, E.M. *Fluid Mechanics. Course of Theoretical Physics*, V. 3. M.: Gostechizdat. 1944. 624 p. (in Russian).
- [6] Baidulov, V. G. & Chashechkin Yu. D. Comparative analysis of symmetries for the models of mechanics of nonuniform fluids. *Doklady Physics*, Vol. 59, No. 5. (2012) pp. 192–196.
- [7] Chashechkin, Yu. D. Hierarchy of models of classical mechanics of inhomogeneous fluids. *J. Physical Oceanography*, Vol. 20, No. 5. (2011) pp. 317–324.
- [8] Chashechkin, Yu. D. & Zagumennyi, Ya. V. Fine structure of unsteady diffusion-induced flow over a fixed plate. *Fluid dynamics*, Vol. 48, No. 3. (2013) pp. 374–388.
- [9] Chashechkin, Yu.D., Bardakov, R.N. & Zagumennyi, Ia.V. Numerical analysis and visualization of fine structures of the fields of two-dimensional internal waves. *J. Physical Oceanography*, Vol. 20, No. 6. (2011) pp. 397–409.
- [10] Chashechkin Yu.D. Differential fluid mechanics: consistent analytical, numerical and laboratory models of stratified flows. *Herald of the Bauman Moscow State Technical University*, Vol. 6, No. 57. (2014) pp. 67–95. (in Russian).